Modeling and robust control of winding systems for elastic webs

Article *in* IEEE Transactions on Control Systems Technology · April 2002

DOI: 10.1109/87.987065 · Source: IEEE Xplore

4 authors:

Hazal Koç
Dumlupinar University
9 PUBLICATIONS **542** CITATIONS
SEE PROFILE

Dominique Knittel
University of Strasbourg
109 PUBLICATIONS **1,537** CITATIONS
SEE PROFILE

Michel De Mathelin
University of Strasbourg
284 PUBLICATIONS **6,688** CITATIONS
SEE PROFILE

Gabriel Abba
École Nationale d'Ingénieurs de Metz
153 PUBLICATIONS **3,730** CITATIONS
SEE PROFILE

Modeling and Robust Control of Winding Systems for Elastic Webs

Hakan Koç, Dominique Knittel, Michel de Mathelin, and Gabriel Abba

***Abstract*—The objective is to control a web transport system with winder and unwinder for elastic material. A physical modeling of this plant is made based on the general laws of physics. For this type of control problem, it is extremely important to prevent the occurrence of web break or fold by decoupling the web tension and the web velocity. Due to the wide-range variation of the radius and inertia of the rollers the system dynamics change considerably during the winding/unwinding process. Different strategies for web tension control and linear transport velocity control are presented in this paper. First, a H_∞ robust control strategy which reduces the coupling between tension and velocity, is compared to the decentralized control strategy with proportional integral derivative (PID) controllers commonly used in the industry. Second, a H_∞ robust control strategy with varying gains is shown to render the control more robust to the radius variations. Then, a linear parameter varying (LPV) control strategy with smooth scheduling of controllers is synthesized for different operating points and compared to the previous methods. Finally, this LPV control and the H_∞ robust control strategy with varying gains are combined to give the best results on an experimental setup, for the rejection of the disturbances introduced by velocity variations and for the robustness to radius and inertia changes.**

***Index Terms*—Gain-scheduling, linear matrix inequality (LMI)-based control design, linear parameter varying (LPV) control, robust H_∞ control, web transport, winding process.**

I. Introduction

SYSTEMS transporting paper, metal, polymers or fabric are quite common in the industry. The main objective in industrial applications is to increase as much as possible the web transport velocity while controlling the tension of the web. Generally, the control of the industrial production is based on simple proportional integral derivative (PID) control techniques and on the know-how of the operators. However, this approach becomes unsatisfying at high velocity and with thin material.

There exist many sources of disturbances on the velocity, e.g., roller noncircularity, roller change, web sliding. Due to the strong coupling between web velocity and web tension, introduced by the elastic web, these disturbances are transmitted to the web tension. The variation of web tension can result in a web break or fold. In case of web break or fold the production line stops, resulting in a waste of time and a lower productivity.

Several studies about standard control techniques in the web handling domain can be found, e.g., in [1]–[3]. A decoupling technique is proposed in [4] for a metal transport line. Note that multivariable control strategies have been recently proposed for industrial metal transport systems (see, e.g., [5] and [6]), and an H_∞ robust control strategy is presented in [7] for the decoupling of web tension and velocity. A fault tolerant control strategy has also been recently presented in [8].

Another concern is the robustness to the variation of the radius and the inertia of the rollers during the winding process. Since the synthesis of the multivariable controller is made for a particular operating point, the controller is not well tuned for all the winding process. This paper presents different approaches to improve robustness to the change of the radius and inertia during the winding process. The first approach is based on a special property of the plant and consists in using the radius of the rollers as proportional gains in the control law. The second approach, is based on linear parameter varying (LPV) control. The third one combines the two first approaches: LPV control with varying gains depending on the radius. Theses approaches significantly improve the performance and robustness compared to classical PID control.

The system under study has three motors (cf. Fig. 1) and exhibits the inherent problems of elastic web transport systems. The experimental setup has been realized at Strasbourg I University for high-speed winding of elastic material (500 m/min) and is used for all our experiments. It should be noted that all the results presented in this paper have been validated on the experimental setup. The parameters of the experimental setup are given in the Appendix.

The first section of this paper presents the modeling of the plant. In the following section, the model is identified through a multistep procedure using optimization algorithms. The third section shows the improvement of the control performances brought by a multivariable robust controller compared to the standard PID control strategy. In the fourth section, a gain scheduling approach is added to the robust control law to minimize the effect of roller radius variations during the winding process. In the following section an LPV controller is designed (see [9]–[11]). This controller is a convex decomposition of H_∞ controllers obtained for different operating points. Finally, in the last section the LPV control strategy with varying gains depending on the radius is presented.

Manuscript received August 14, 2000. Manuscript received in final form August 16, 2001. Recommended by Associate Editor E. G. Collins, Jr. This work was supported by the French Ministry of Research under ERT-Project "High-speed handling and winding of flexible webs."

H. Koç is with Siemens AG, A&D MC PM 5, 91056 Erlangen, Germany.

D. Knittel and M. de Mathelin are with Strasbourg I University, ERT Enroulement-LSIIT UMR CNRS 7005, ENSPS, Bd. S. Brant, 67400 Illkirch, France (e-mail: dominique.knittel@ipst-ulp.u-strasbg.fr).

G. Abba is with the University of Metz, IUT Espace Cormantaigne, 57970 Yutz, France.

Publisher Item Identifier S 1063-6536(02)00333-0.

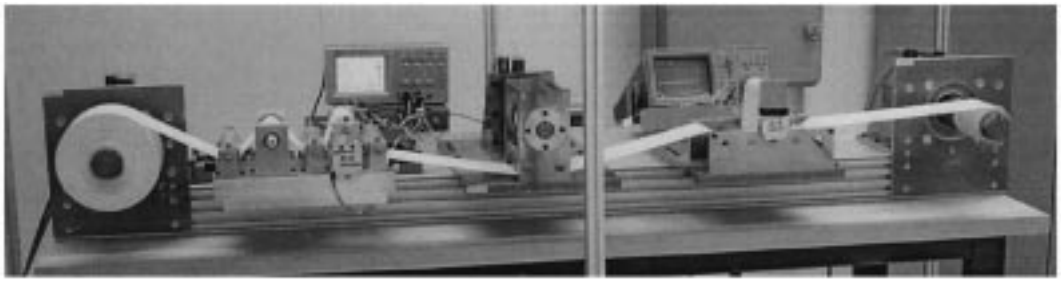

Fig. 1. Experimental setup.

II. Modeling

The model of a web transport system is built using the model of the web tension between two consecutive rolls and the dynamical model of the velocity of each roll.

A. Web Tension Between Two Consecutive Rolls

The different models for the web tension in web transport systems are based on three laws [12]:

- *Hooke's law*, which models the elasticity of the web;
- *Coulomb's law*, which gives the web tension variation due to friction and to the contact force between web and roll;
- *Mass conservation law*, which expresses the cross-coupling between web velocity and web strain.

The web tension between two rolls can be computed based on these three laws.

Hooke's Law: The tension T of an elastic web is function of the web strain ϵ:

$$T = ES\epsilon = ES\,\frac{L - L_0}{L_0} \tag{1}$$

where E is Young's modulus, S is the web section, L is the web length under stress and L_0 is the nominal web length (without stress). Note that the relationship between the strain and the tension is more complex for viscoelastic materials. The Hooke's law is valid for most web materials, as long as the tension is not too large.

Moreover, the Young's modulus is very sensitive to the temperature and the humidity level. On the production line, the web may go through different processes (for example, in a solvent bath, then in a dryer). Therefore, its elasticity properties may considerably change during the process.

Coulomb's Law: The study of the web tension on a roll can be considered as a problem of friction between solids, see [12] and [13]. On the roll, the web tension is constant on a sticking zone which is an arc of length a and varies on a sliding zone which is an arc of length g (cf. Fig. 2). Then, the web strain between the first contact point of a roll and the first contact point of the following roll is given by

$$\epsilon(x,\,t) = \epsilon_1(t) \qquad \text{if } x \le a \tag{2}$$

$$= \epsilon_1(t) e^{\mu(x-a)} \qquad \text{if } a \le x \le a+g \tag{3}$$

$$= \epsilon_2(t) \qquad \text{if } a+g \le x \le L_t \tag{4}$$

where μ is the friction coefficient and $L_t = a + g + L$.

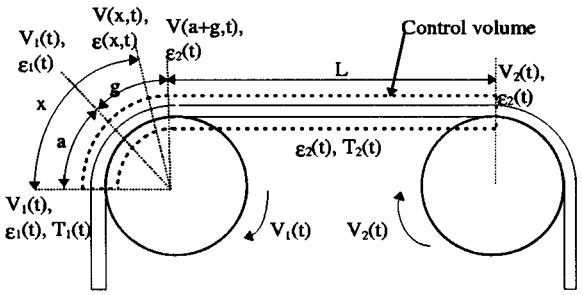

Fig. 2. Web tension on the roll.

The tension change occurs on the sliding zone while the web velocity is equal to the roll velocity on the sticking zone. There can also appear a sliding zone at the roll entry if the tension varies at high rate [12].

Mass Conservation Law: Consider a web of length $L = L_0(1+\epsilon)$ with a weight density ρ, under an unidirectional stress. Assuming that the cross section stays constant, then, according to the mass conservation law, the mass of the web remains constant between the state without stress and the state under stress

$$\rho S L = \rho_0 S L_0 \qquad \Rightarrow \qquad \frac{\rho}{\rho_0} = \frac{1}{1+\epsilon}. \tag{5}$$

Web Tension Between Two Consecutive Rolls: The equation of continuity applied to the web transport system gives, cf. [12]

$$\frac{\partial \rho}{\partial t} + \frac{\partial(\rho V)}{\partial x} = 0 \tag{6}$$

where V represents the web velocity in the control volume. Using (5), we integrate on the control volume $\mathcal{V}$ defined by the first contact points between the web and the rolls, see Fig. 2

$$\int_{\mathcal{V}} \frac{\partial}{\partial t}\left(\frac{1}{1+\epsilon}\right) d\mathcal{V} = -\int_{\mathcal{V}} \frac{\partial}{\partial x}\left(\frac{V}{1+\epsilon}\right) d\mathcal{V}. \tag{7}$$

Assuming that the web section is constant, $d\mathcal{V} = S\,dx$, we can integrate with respect to the variable x from zero to L_t

$$\frac{\partial}{\partial t}\left(\int_0^{L_t} \frac{1}{1+\epsilon(x,\,t)}\,dx\right) = -\int_0^{L_t} \frac{\partial}{\partial x}\left(\frac{V(x,\,t)}{1+\epsilon(x,\,t)}\right) dx. \tag{8}$$

Using (2)–(4) and assuming that $a + g \ll L$, we obtain, see [14] and [15], that

$$\int_0^{L_t} \frac{1}{1+\epsilon(x,\,t)}\,dx \simeq \frac{L}{1+\epsilon(L_t,\,t)}. \tag{9}$$

Let $\epsilon(0,t) = \epsilon_1$, $\epsilon(L_t,t) = \epsilon_2$, $V(0,t) = V_1$ and $V(L_t,t) = V_2$, then, the final relationship is

$$\frac{d}{dt}\left(\frac{L}{1+\epsilon_2}\right) = \frac{V_1}{1+\epsilon_1} - \frac{V_2}{1+\epsilon_2}. \tag{10}$$

This relationship can be simplified by differentiating the left term

$$-L\frac{d\epsilon_2}{dt} = V_1\frac{(1+\epsilon_2)^2}{1+\epsilon_1} - V_2(1+\epsilon_2). \tag{11}$$

Then, using the approximations

$$\epsilon_1 \ll 1, \quad \epsilon_2 \ll 1, \quad \frac{(1+\epsilon_2)^2}{1+\epsilon_1} \approx (1-\epsilon_1)(1+2\epsilon_2)$$

and (1), we obtain

$$L\frac{dT_2}{dt} \simeq ES(V_2 - V_1) + T_1V_1 - T_2(2V_1 - V_2). \tag{12}$$

This relationship differs from that presented in classical studies (e.g., [1], [16]) on winding systems. The classical model simplification is obtained by using the approximation before differentiating the left term in (10), and gives the following equation:

$$L\frac{dT_2}{dt} \simeq ES(V_2 - V_1) + T_1V_1 - T_2V_2. \tag{13}$$

This equation is equivalent to our relationship (12) if $V_2 = V_1$. Fig. 3 shows the web strain under velocity variations. We can see that (12) gives a better approximation than (13). This improvement is mainly relevant for simulation purpose.

B. Web Velocity on Each Roll

Assuming that the web does not completely slide on the roll, the web velocity is equal to the roll linear velocity. The velocity V_k of the kth roll can be obtained through a torque balance

$$\frac{d(J_k\Omega_k)}{dt} = R_k(T_{k+1} - T_k) + K_kU_k + C_f \tag{14}$$

where $\Omega_k = V_k/R_k$ is the rotational speed of roll k, K_kU_k is the motor torque (if the roll is driven), J_k is the roll inertia, R_k is the roll radius and C_f is the sum of the friction torques. We can notice at this point that the inertia J_k and the radius R_k are time dependent: J_k and R_k increase with time at the winder and decrease with time at the unwinder. They may vary greatly during the complete process operation (about 300% for the radius in our experimental setup and even more in some industrial systems).

C. Linearized Model

The complete model of our experimental setup can be built using (10) to specify the tension in each span and equation (14) to specify the velocity of each roll. To synthesize the controllers we need a linearized model of the plant. The linear model is obtained by linearizing the simplified form of the equations around the nominal web tension and velocity, by assuming slow variations of the radius and inertia and by considering only viscous

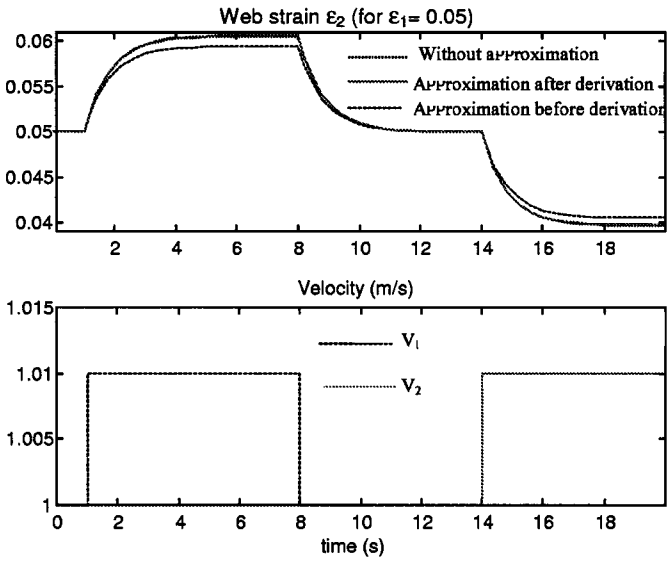

Fig. 3. Web strain under velocity variations.

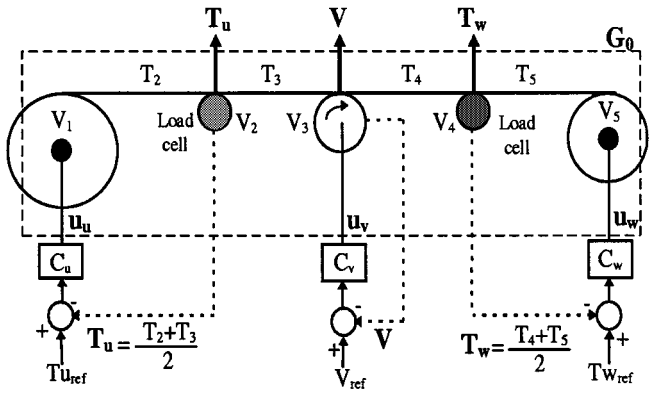

Fig. 4. Decentralized control.

friction torques. If V_0 and T_0 are, respectively, the nominal web velocity and tension then, the relationship (12) becomes

$$L\frac{dT_2}{dt} = (ES + T_0)(V_2 - V_1) + V_0(T_1 - T_2). \tag{15}$$

Fig. 4 shows the different variables in the nominal model G_0 of our experimental system. The inputs are the control signals u_u, u_v and u_w and the outputs are the unwinding web tension T_u, traction motor's linear velocity V, and winding web tension T_w. Notice that, before computing the control signals each measured output signal is filtered with a first-order filter. The control signals are the reference torque of synchronous motors. Traditionally, in a decentralized control scheme, the web velocity is controlled by the traction motor and the web tension is controlled by the unwinding and winding motors. Using (14) and (15), the state-space representation of the nominal model around an operating point, $V_i = V_0$, for $i \in [1, \ldots, 5]$, $T_i = T_0$, for $i \in [2, \ldots, 5]$ (with a web tension on the unwound roller equal to zero, $T_1 = 0$) can be expressed as

$$E_m\dot{X} = A(t)X + BU$$

$$Y = CX$$

where as shown in the equations at the bottom of the page, V_i, Ω_i, R_i, J_i, and f_i are, respectively, the linear velocity, the rotational speed, the radius, the inertia, and the viscous friction coefficient of the roll i, where T_i, and L_i are, respectively, the web tension and the web length between the roll $i-1$ and the roll i, where K_u, K_t and K_w are the torque constants of each motor, and E_0 is a constant depending on the elasticity modulus and the section of the web, $E_0 = ES + T_0$. The parameters varying during the winding process are expressed as function of time.

III. Identification

The identification of the complete nonlinear parametric model including three motors and two load cells is based on the model matching approach. It is done in several steps in order to reduce the number of parameters to identify at each step and, consequently, simplify the optimization of the parameters. The first step consists in identifying the friction torque of each motor by using a least squares method with data acquired at constant speed. At constant speed, the friction model of each motor can be identified without the knowledge of the inertia and the torque constant. The second step is based on the model matching method (see Fig. 5) applied to a system with two motors (unwinder and winder) and one load cell, with the friction models identified in the first step.

The rolls of the load cell are modeled by a single roll with an inertia to be identified. The inertia of the motors and the load cells' rolls and the torque gains [K_k in (14)] are identified by parameter optimization. The last step consists in identifying the remaining parameters of the complete model by optimization. The cost function used in the optimization is of the following form:

$$J_{opt} = \frac{(Y_s - Y_m)^T (Y_s - Y_m)}{\|Y_m\|^2} \tag{16}$$

$$X^T = \begin{pmatrix} J_1\Omega_1 & T_2 & V_2 & T_3 & V_3 & T_4 & V_4 & T_5 & J_5\Omega_5 \end{pmatrix}$$

$$U^T = \begin{pmatrix} u_u & u_v & u_w \end{pmatrix}, \quad Y^T = \begin{pmatrix} \dfrac{T_2+T_3}{2} & V_3 & \dfrac{T_4+T_5}{2} \end{pmatrix} = \begin{pmatrix} T_u & V & T_w \end{pmatrix}$$

$$A(t) = \begin{bmatrix} -\dfrac{f_1(t)}{J_1(t)} & R_1(t) & 0 & 0 & 0 & 0 & 0 & 0 & 0 \\ -E_0\dfrac{R_1(t)}{J_1(t)} & -V_0 & E_0 & 0 & 0 & 0 & 0 & 0 & 0 \\ 0 & -R_2^2 & -f_2 & R_2^2 & 0 & 0 & 0 & 0 & 0 \\ 0 & V_0 & -E_0 & -V_0 & E_0 & 0 & 0 & 0 & 0 \\ 0 & 0 & 0 & -R_3^2 & -f_3 & R_3^2 & 0 & 0 & 0 \\ 0 & 0 & 0 & V_0 & -E_0 & -V_0 & E_0 & 0 & 0 \\ 0 & 0 & 0 & 0 & 0 & -R_4^2 & -f_4 & R_4^2 & 0 \\ 0 & 0 & 0 & 0 & 0 & V_0 & -E_0 & -V_0 & E_0\dfrac{R_5(t)}{J_5(t)} \\ 0 & 0 & 0 & 0 & 0 & 0 & 0 & -R_5(t) & -\dfrac{f_5(t)}{J_5(t)} \end{bmatrix},$$

$$E_m = \begin{bmatrix} 1 & 0 & 0 & 0 & 0 & 0 & 0 & 0 & 0 \\ 0 & L_1 & 0 & 0 & 0 & 0 & 0 & 0 & 0 \\ 0 & 0 & J_2 & 0 & 0 & 0 & 0 & 0 & 0 \\ 0 & 0 & 0 & L_3 & 0 & 0 & 0 & 0 & 0 \\ 0 & 0 & 0 & 0 & J_3 & 0 & 0 & 0 & 0 \\ 0 & 0 & 0 & 0 & 0 & L_3 & 0 & 0 & 0 \\ 0 & 0 & 0 & 0 & 0 & 0 & J_4 & 0 & 0 \\ 0 & 0 & 0 & 0 & 0 & 0 & 0 & L_4 & 0 \\ 0 & 0 & 0 & 0 & 0 & 0 & 0 & 0 & 1 \end{bmatrix}, \quad B = \begin{bmatrix} -K_u & 0 & 0 \\ 0 & 0 & 0 \\ 0 & 0 & 0 \\ 0 & 0 & 0 \\ 0 & K_tR_3 & 0 \\ 0 & 0 & 0 \\ 0 & 0 & 0 \\ 0 & 0 & 0 \\ 0 & 0 & K_w \end{bmatrix}$$

$$C = \begin{bmatrix} 0 & \frac{1}{2} & 0 & \frac{1}{2} & 0 & 0 & 0 & 0 & 0 \\ 0 & 0 & 0 & 0 & 1 & 0 & 0 & 0 & 0 \\ 0 & 0 & 0 & 0 & 0 & \frac{1}{2} & 0 & \frac{1}{2} & 0 \end{bmatrix}$$

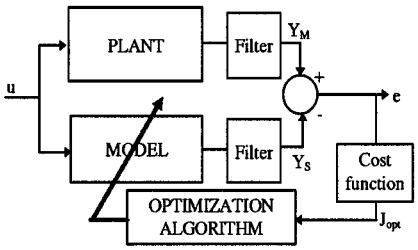

Fig. 5. Model matching method.

where Y_s, Y_m are, respectively, the vectors of simulated and measured output signals T_u, V and T_w (see Fig. 4). We assume that there are no sliding effects between the web and the roller, i.e., there exists always a sticking zone. Therefore, the web velocity is equal to the roll velocity. Two optimization algorithms have been used: the simplex method (Nelder and Mead) and the quasi-Newton method, cf. [17].

Note that other methods of identification are presented, e.g., in [18], based on a black box modeling of the winding system.

In Fig. 6, simulations of the model with the optimized parameters are compared to the measurements obtained on the experimental setup. We observe a closed match between the simulations and the measurements. The measurements are obtained with operating conditions guaranteeing the hypothesis of a nonsliding web.

IV. Robust H_∞ Control

Robust H_∞ control is a powerful tool to synthesize multivariable controllers with interesting properties of robustness and disturbances rejection. The synthesis of the multivariable controller is done using the nominal model G_0 (see Fig. 4). The nominal model is chosen with the radius and inertia corresponding to the starting phase, i.e., full roller at the unwinder and empty roller at the winder. The starting phase is very important: if a problem occurs in this phase, most likely, the roller will be badly wounded. Then, the controller should always guarantee a good starting phase. To do so, the velocity must be kept equal to zero during the increase in tension of the web and the tension oscillations during the increase in speed of the web must be rejected.

The robust H_∞ controller is synthesized using the mixed sensitivity approach (cf. [19] and [20]), as shown in Fig. 7, where w are the exogenous inputs and z are the controlled signals.

The frequency weighting functions W_p, W_u and W_t appear in the closed-loop transfer function matrix in the following manner:

$$T_{wz} := \begin{bmatrix} W_p\mathcal{S} \\ W_uK\mathcal{S} \\ W_t\mathcal{T} \end{bmatrix} \tag{17}$$

where $\mathcal{S}$ is the sensitivity function, $\mathcal{S} = (I + GK)^{-1}$, and $\mathcal{T}$ is the complementary sensitivity function $\mathcal{T} = I - \mathcal{S}$.

The controller K is calculated using "γ-iterations" [21, Doyle–Glover algorithm]. It is a stabilizing controller such that the H_∞ norm of the transfer function between w and z is

$$||T_{wz}||_\infty := \sup_w \sigma_{\max}(T_{wz}(jw)) \le \gamma \tag{18}$$

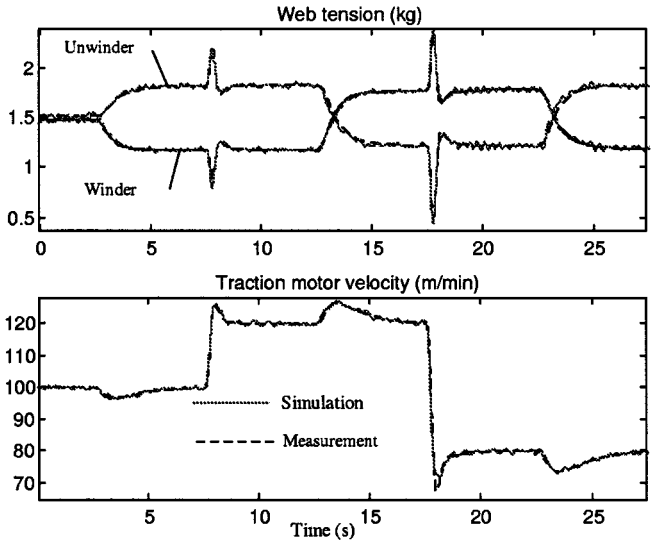

Fig. 6. Identification results.

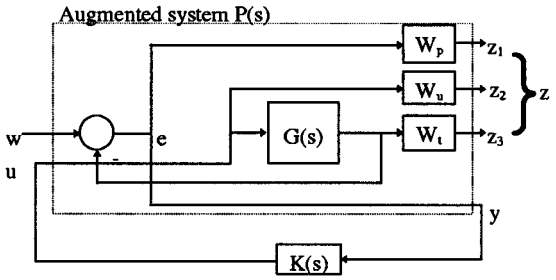

Fig. 7. Mixed sensitivity method.

with γ close to $\gamma_{\min}$, the smallest possible value of γ. In a sense, the controller K "minimizes" the transfer between w and the controlled signals z.

The frequency weighting function W_p is usually selected with a high gain at low frequency to reject low-frequency perturbations and to reduce steady-state error. The structure of W_p is as follows (cf. [19] and [22]):

$$W_p(s) = \frac{\frac{s}{M} + w_B}{s + w_B\epsilon_0} \tag{19}$$

where M is the maximum peak magnitude of $\mathcal{S}$, $||\mathcal{S}||_\infty \le M$, w_B is the required bandwidth frequency and ϵ_0 is the steady-state error allowed. The weighting function W_u is used to avoid large control signals and the weighting function W_t increases the roll-off at high frequencies.

The selected weighting functions in our experiments are

$$W_p(s) = \begin{bmatrix} \frac{0.5s+11}{s+0.01} & 0 & 0 \\ 0 & \frac{0.5s+9}{s+0.01} & 0 \\ 0 & 0 & \frac{0.5s+11}{s+0.01} \end{bmatrix}$$

$$W_u = I_{3\times 3}; \qquad W_t(s) = \begin{bmatrix} 2s & 0 & 0 \\ 0 & s & 0 \\ 0 & 0 & 2s \end{bmatrix}.$$

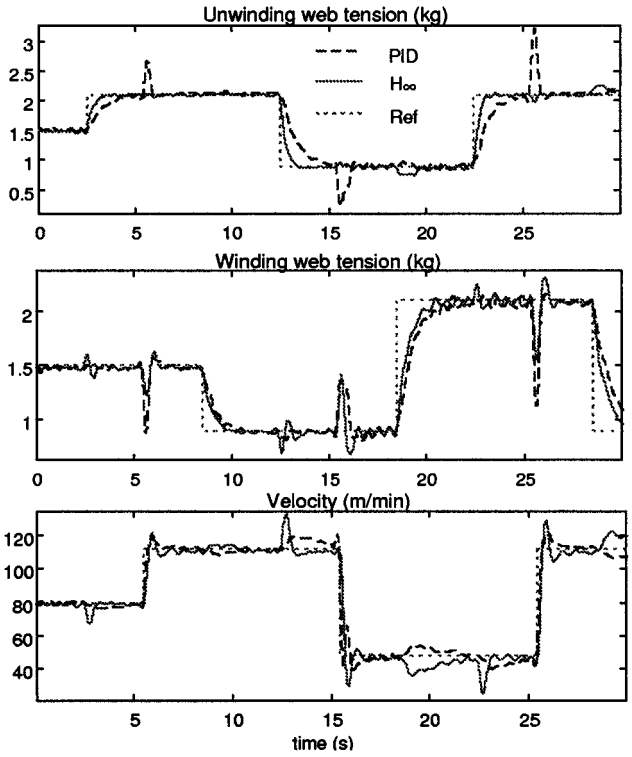

Fig. 8. PID versus H_∞ control.

The pole in the weighting function W_p is an almost integrator to avoid numerical problem, cf. [19]. The weighting function W_t has no pole and, consequently, does not increase the order of the controller. The order of the resulting controller is 15. An analysis of the Hankel singular values shows that the reduction of the controller order is not recommended. The controller has been implemented on the experimental setup in state space representation with a sampling period of 10 ms.

The decentralized control using PID controllers and the multivariable H_∞ robust control are compared on Fig. 8 in real experiments. The improvement of the unwinding web tension control is very significant with the H_∞ controller. The web tension is maintained constant during the change of velocity. However, the improvement on the winding tension control is not as important. We observe that a change in the unwinding tension has some effects on the winding tension, whereas a change in the winding tension does not have any effect on the unwinding tension even with PID controllers. That shows the transmissibility of the tension (cf. [15] and [16]) and the fact that the winding tension is more difficult to control than the unwinding tension. Finally, we do not observe any improvement of the control of the velocity with the H_∞ controller. The main reason is that the nominal model (corresponding to the starting phase) considered in this H_∞ controller synthesis does not follow closely enough the dynamics of the system during all the winding process.

V. Robust H_∞ Control With Varying Gains Depending on the Radius

Considering the unwinder and the winder separately, if the time varying parameters J_i and R_i were constant, the transfer function between the control signals and the web tensions could be written as

$$\frac{T_2(s)}{u_u(s)} = \frac{K_u R_1 E_0}{J_1 L_1 s^2 + (J_1 V_0 + L_1 f_1)s + f_1 V_0 + R_1^2 E_0} \quad (20)$$

$$\frac{T_5(s)}{u_w(s)} = \frac{K_w R_5 E_0}{J_5 L_4 s^2 + (J_5 V_0 + L_4 f_5)s + f_5 V_0 + R_5^2 E_0}. \quad (21)$$

In most cases, $E_0 \gg 1$, and $R_i^2 E_0 \gg f_i V_0$ for $i \in [1, 5]$ and for all admissible values of the radius. Using this approximation, we can see that the dc gains of the transfer functions are inversely proportional to the radius:

$$\lim_{s\to 0} \frac{T_2(s)}{u_u(s)} \simeq \frac{K_u}{R_1} \qquad \lim_{s\to 0} \frac{T_5(s)}{u_w(s)} \simeq \frac{K_w}{R_5}. \quad (22)$$

Based on this observation, we propose to multiply the controller output signals by the respective radius in order to make the dc gains independent of the radius. A simulation of the system with and without the multiplication by the radius (gain scheduling) using PID controllers shows that the gain scheduling makes the steady-state error equal to zero and keeps the performance similar (overshoot and time response) during all the process run, (see Fig. 9). Fig. 10 shows the modified system.

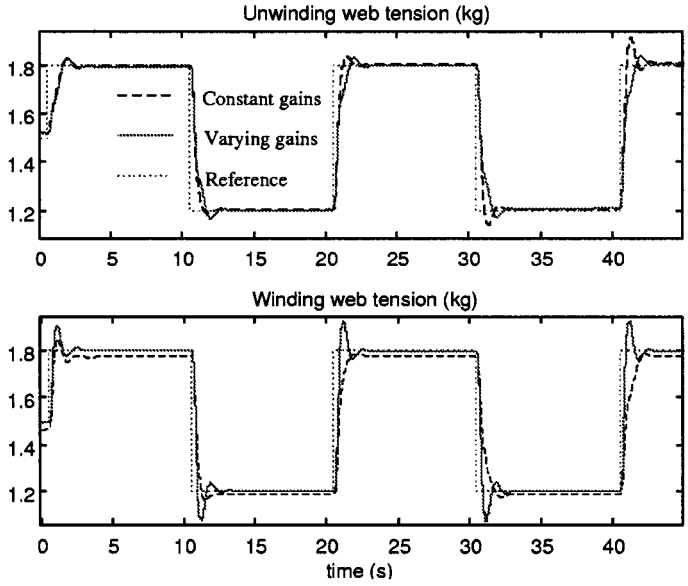

Fig. 9. Simulation: PID with gain scheduling.

The improvement with this gain scheduling is significant with PID controllers. To take advantage of this property in a multivariable control strategy a new nominal plant G_R is obtained by multiplying the controller output signals v_u and v_w by the radius R_u (=R_1) et R_w (=R_5), respectively (see Fig. 11). This new plant has the advantage of making the gains [cf. relation (22)] at low frequency less dependent of the radius and inertia. Fig. 11 shows the maximum singular values of the nominal systems G_0 and G_R at different operating points with different radius and inertia. One can see that the frequency response change less with the radius in the gain scheduling strategy.

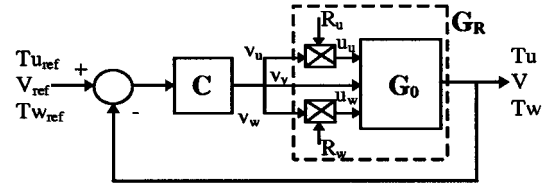

Fig. 10. Modified system.

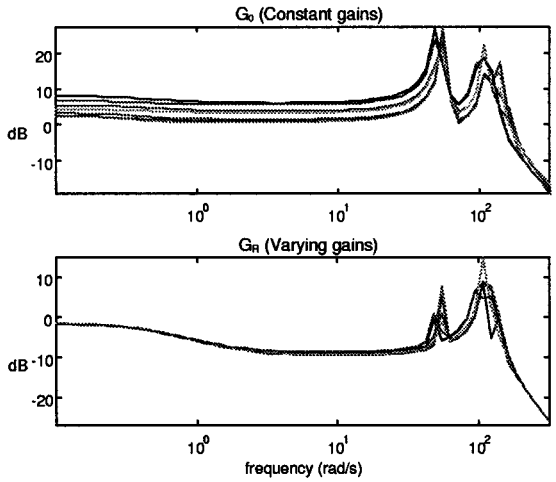

Fig. 11. Maximum singular values for different radius.

For the H_∞ robust control synthesis based on the nominal system G_R, the selected weighting functions are

$$W_p(s) = \begin{bmatrix} \dfrac{0.5s+10}{s+0.01} & 0 & 0 \\ 0 & \dfrac{0.5s+5}{s+0.01} & 0 \\ 0 & 0 & \dfrac{0.5s+10}{s+0.01} \end{bmatrix}$$

$$W_u = I_{3\times 3}; \qquad W_t(s) = \begin{bmatrix} s & 0 & 0 \\ 0 & 2s & 0 \\ 0 & 0 & s \end{bmatrix}.$$

The measurements acquired with the controller based on G_0 are compared to those obtained with the varying gain controller based on G_R. It is shown in Fig. 12 that the controller with varying gains keeps the same performance for reference tracking of the winding web tension and the same response to the perturbation introduced by the velocity variations, during all the process operation.

Furthermore, the varying gain H_∞ controller is less sensitive to the nominal model used in the synthesis of the controller. The behavior of the H_∞ controllers is tested by putting the web under stress in a different condition than the starting phase: e.g., by rewinding. With an empty roller at the unwinder and a full roller at the winder, we put under stress the web while maintaining the velocity equal to zero. It can be seen in Fig. 13 that the velocity does not stay equal to zero and the web tensions oscillate with the constant gain controller. This oscillation of the web tension could result in a break of the web in some cases.

The varying gain H_∞ controller is quite satisfying. However, by looking more precisely to the response of the web tension

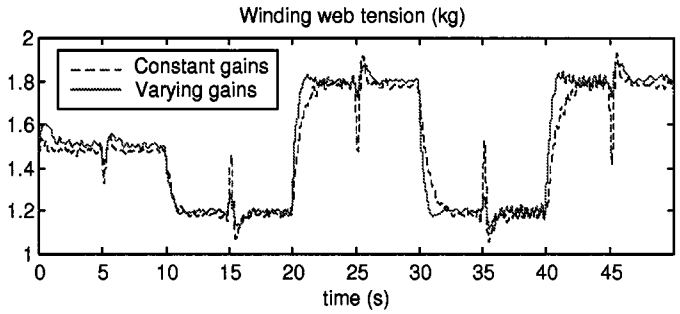

Fig. 12. Comparison of winding web tensions with and without gain scheduling multivariable control.

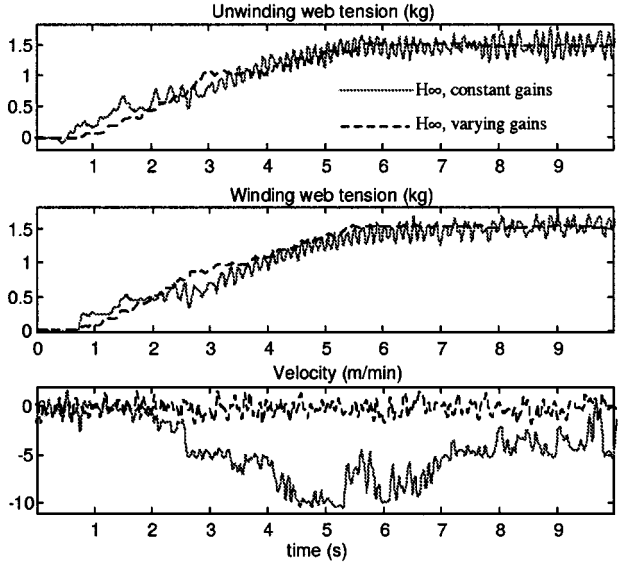

Fig. 13. Comparison between constant and varying gain controls: rewinding.

to quasiperiodical velocity variations (as it is always present in winding process), a decrease of the performance for disturbance rejection is observed in Fig. 16. Moreover the variations of the singular values of the system G_R (see Fig. 11) become more and more important when the frequency increases. Thus, the larger the bandwidth the higher is the influence of the radius and inertia.

The next step will consist in looking for a controller which guarantees the same performance during all the process run. The solution to this problem consists in computing a controller for different operating points and making a smooth scheduling between controllers.

VI. LPV Control

The synthesis of LPV controller using the linear matrix inequalities (LMIs) techniques offers the possibility of taking into consideration a very large uncertainty. The performance of the controller can be increased by a robust gain scheduling controller. Moreover, the synthesis of a robust controller without varying parameter by LMI resolution encompass also the classical H_∞ synthesis. Furthermore, the LMI techniques are more general and allow to suppress some drawbacks of the H_∞ control. The main advantages of the LMI-based approach are

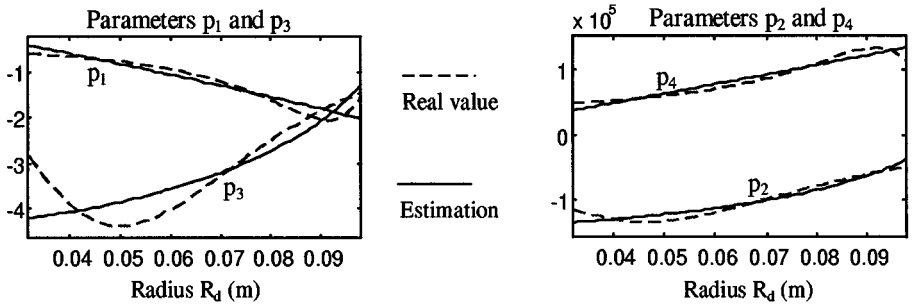

Fig. 14. Linear approximation.

- suppression of the regularity restriction attached to the Riccati equations resolution of the H_∞ synthesis,
- multiobjective H_∞ synthesis (e.g., mixed H_2/H_∞ synthesis with a placement of the closed-loop poles in a prescribed LMI region),
- the possibility to take into consideration the order of the controller in the synthesis.

A. LPV Representation of the Plant

We consider the augmented plant, $P(\theta)$, a parameter-dependent system, where the parameters, $\theta^T = [R_1(t)\, R_5(t)]$ are time varying. We assume that the other time varying parameters f_1/J_1, R_1/J_1, f_5/J_5 and R_5/J_5 appearing in the matrix A of the state-space representation given in Section II-C can be expressed approximately affinely in function of the radius $R_1 = R_d$ and R_5. Let $p_1 = f_1/J_1$, $p_2 = R_1/J_1$, $p_3 = f_5/J_5$ and $p_4 = R_5/J_5$, then

$$p_i = \lambda_{1i} R_1 + \lambda_{5i} R_5 \quad \text{for} \quad i \in [1, \ldots, 4] \tag{23}$$

where the coefficients λ_{1i} and λ_{5i} are obtained through least squares approximation as shown in Fig. 14.

With the notation w for exogenous input signals, u for the control signals, z for controlled variables and y for the measured signals, the plant $P(\theta)$ can be written as following:

$$\begin{aligned} \dot{x} &= A(\theta)x + B_1(\theta)w + B_2(\theta)u \\ z &= C_1(\theta)x + D_{11}(\theta)w + D_{12}(\theta)u \\ y &= C_2(\theta)x + D_{21}(\theta)w + D_{22}(\theta)u \end{aligned} \tag{24}$$

where $A(\theta)$, $B_i(\theta)$, $C_i(\theta)$ and $D_{ij}(\theta)$ are functions of the time varying parameter $\theta(t)$ in a polytopic set $\mathcal{P}_\theta$, i.e.,

$$\theta(t) \in \mathcal{P}_\theta := Co\{\theta_1, \theta_2, \theta_3, \theta_4\} \tag{25}$$

the notation $Co\{.\}$ stands for the convex hull of the set $\{.\}$. Given any convex decomposition of the parameter θ, i.e.,

$$\theta(t) = \alpha_1\Pi_1 + \alpha_2\Pi_2 + \alpha_3\Pi_3 + \alpha_4\Pi_4$$
$$\alpha_i \geq 0 \text{ for } i \in [1, \ldots, 4], \qquad \sum_{i=1}^{i=4} \alpha_i = 1 \tag{26}$$

where the Π_i, for $i \in [1, \ldots, 4]$, correspond to the corners of the parameter box as shown in Fig. 15 (indeed, the radius of each roller varies always between a $R_{\min}$ and a $R_{\max}$ values).

A parameter-dependent controller is sought with the same vertex property

$$K(\theta) = \alpha_1 K(\Pi_1) + \alpha_2 K(\Pi_2) + \alpha_3 K(\Pi_3) + \alpha_4 K(\Pi_4). \tag{27}$$

The synthesis of the controller is done as in a H_∞-like synthesis problem, so that (cf. [11] and [23]):

- the closed-loop system is stable for all admissible trajectories $\theta(t)$,
- the L_2-induced gain of the operator connecting w to z is bounded by γ.

This synthesis problem can be reduced to the following LMI problem (under the assumption that B_2, C_2, D_{12}, and D_{21} are parameter-independent, see [24]): find a pair of symmetric matrices (X, Y) satisfying the LMI conditions for $i \in \{1, \ldots, 4\}$

$$\begin{aligned} &\mathcal{N}_\mathcal{X}^T \begin{pmatrix} A_iX + XA_i & XB_{1i} & C_{1i}^T \\ B_{1i}^T X & -\gamma I & D_{11i}^T \\ C_{1i} & D_{11i} & -\gamma I \end{pmatrix} \mathcal{N}_\mathcal{X} < 0 \\ &\mathcal{N}_\mathcal{Y}^T \begin{pmatrix} A_iY + YA_i^T & YC_{1i} & B_{1i} \\ C_{1i}X & -\gamma I & D_{11i} \\ B_{1i}^T & D_{11i}^T & -\gamma I \end{pmatrix} \mathcal{N}_\mathcal{Y} < 0 \\ &\qquad\qquad \begin{pmatrix} X & I \\ I & Y \end{pmatrix} > 0 \end{aligned} \tag{28}$$

where $\mathcal{N}_\mathcal{X}$ and $\mathcal{N}_\mathcal{Y}$ are bases of the null spaces $[B_2^T, D_{12}^T]$ and $[C_2^T, D_{21}^T]$, respectively.

B. LPV Controller Synthesis

The state-space representation of our system given in Section II-C satisfies the requirement on the parameter-independence of the matrices B_2, C_2, D_{12}, and D_{21}. For our application, the synthesis from the LMI problem (28) does not give satisfying controllers. The simulation with the resulting LPV controller gives nonminimum phase-like responses. This synthesis with the quadratic performance condition is too conservative and the optimum γ obtained in this manner, is much larger than the one obtained with the classical H_∞ synthesis. Indeed, in practice R_1 is not independent of R_5 and the parameters values are close to the trajectory drawn in Fig. 15.

Since the controller can not be easily computed directly by the resolution of the LMI problem (28), our approach consists in synthesizing several H_∞ controllers, then, analyzing the quadratic stability of the resulting controller. The controllers $K(\Pi_i)$, for $i \in [1, \ldots, 4]$, are computed separately for four H_∞-like problems corresponding to the corners of the

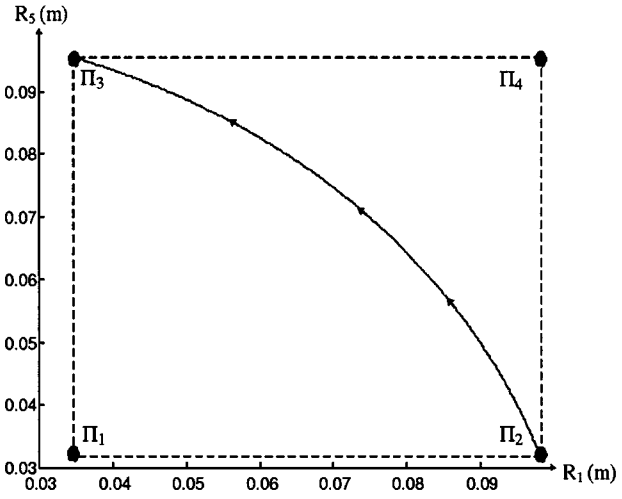

Fig. 15. Parameter trajectory.

parameter box. The same weighting functions are used in the synthesis of each controller. Then, the resulting controller, $K(\theta)$, is obtained using (27) with

$$\alpha_1 = (1-\rho_u)(1-\rho_w) \qquad \alpha_2 = \rho_u(1-\rho_w)$$
$$\alpha_3 = (1-\rho_u)\rho_w \qquad \alpha_4 = \rho_u\rho_w$$

where

$$\rho_u = \frac{R_u(t) - R_{\min}}{R_{\max} - R_{\min}} \qquad \rho_w = \frac{R_w(t) - R_{\min}}{R_{\max} - R_{\min}}$$
$$R_u = R_1 \qquad R_w = R_5$$

then, the controller K is defined as

$$\dot{x}_K = A_K x_K + B_K e$$
$$U = C_K x_K$$

with

$$A_K = \begin{bmatrix} A_{K1} & & & 0 \\ & A_{K2} & & \\ & & A_{K3} & \\ 0 & & & A_{K4} \end{bmatrix} \quad B_K = \begin{bmatrix} B_{K1} \\ B_{K2} \\ B_{K3} \\ B_{K4} \end{bmatrix}$$
$$C_K = [\alpha_1 C_{K1} \quad \alpha_2 C_{K2} \quad \alpha_3 C_{K3} \quad \alpha_4 C_{K4}].$$

Defining the augmented state variable $x_{cl}^T = [x^T \; x_K^T]$, the closed-loop system is obtained from (24) (for $D_{22} = 0$)

$$\dot{x}_{cl} = A_{cl} x_{cl} + B_{cl} w$$
$$z = C_z x_{cl} + D_{11} w$$
$$y = C_y x_{cl} + D_{21} w$$

where

$$A_{cl} = \begin{bmatrix} A & B_2 C_K \\ -B_K C_2 & A_K \end{bmatrix} \quad B_{cl} = \begin{bmatrix} B_1 \\ B_K(I - D_{21}) \end{bmatrix}$$
$$C_z = [C_1 \quad D_{12} C_K] \quad C_y = [C_2 \quad 0].$$

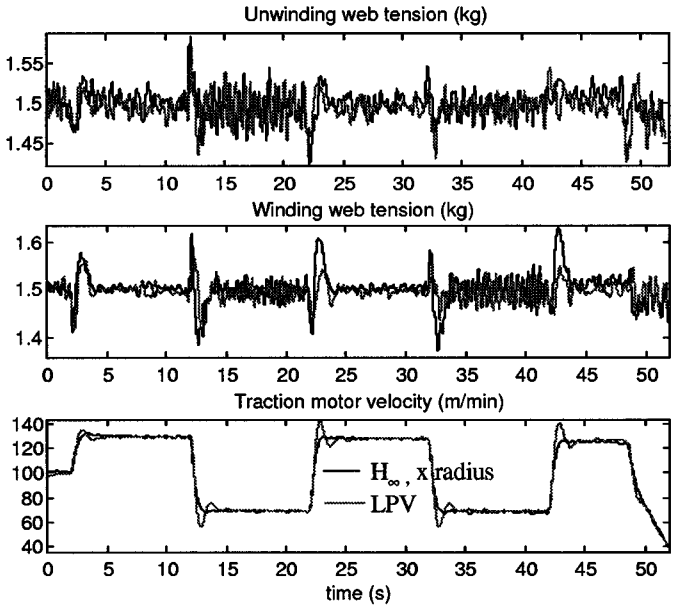

Fig. 16. Web tension for periodical velocity variations.

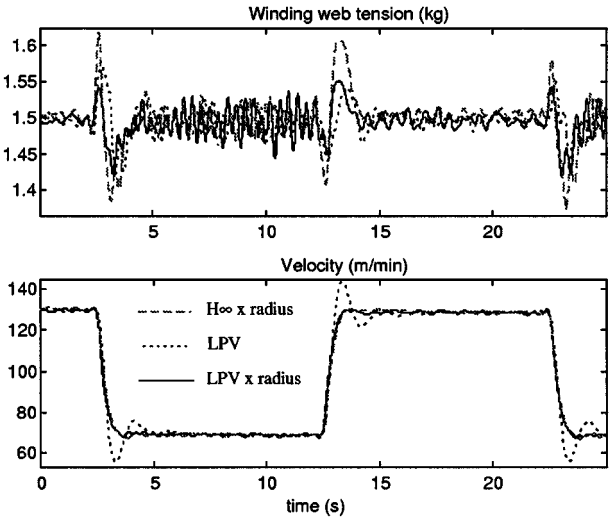

Fig. 17. Comparison of the gain scheduled controllers.

C. Study of the Stability

The considered polytopic system $A_{cl}(t) \in Co\{A_{cl1}, \ldots, A_{cl4}\}$ is quadratically stable if there exist a symmetric matrix Q and scalars $t_{ij} = t_{ji}$ such that (cf. [24] and [25])

$$A_{cli}Q + QA_{cli}^T + A_{clj}Q + QA_{clj}^T < 2t_{ij}I \quad \text{for } i, j \in \{1, \ldots, 4\}$$
$$Q > I$$
$$\begin{bmatrix} t_{11} & \cdots & t_{14} \\ \vdots & \ddots & \vdots \\ t_{14} & \cdots & t_{44} \end{bmatrix} < 0. \tag{29}$$

The proof of the quadratic stability guarantees arbitrary fast time variations, which may be too conservative if the system order is too high. The order of the matrix A_{cl} of our application

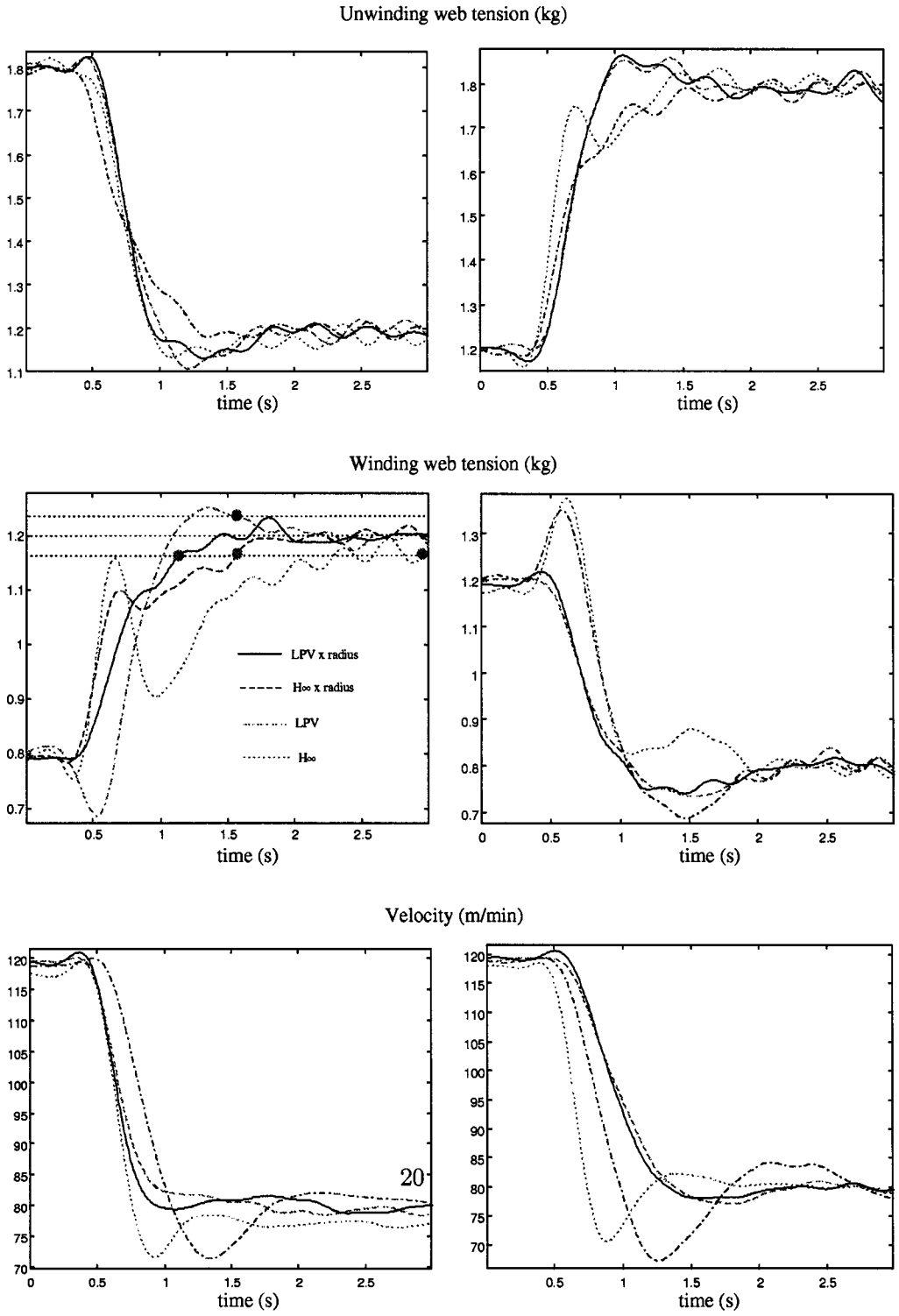

Fig. 18. Comparison of the multivariable controllers.

is 72 which was too large to render the LMI resolution possible. To avoid this problem, the polytopic closed-loop system is computed from the polytopic open-loop system $\mathcal{L}_k = K_i G_{0j}$ for $i, j \in \{1, \ldots, 4\}$ and $k \in \{1, \ldots, 16\}$. The resulting order of the closed-loop system is now 27, but the number of vertices of the polytopic closed-loop system is 16. Then, the quadratic stability of the closed-loop system is verified using the LMI toolbox of Matlab [26]. A solution Q_{opt} and $\tau < 0$ is found such that

$$\begin{aligned} &A_{cli}Q_{\text{opt}} + Q_{\text{opt}}A_{cli}^T + A_{clj}Q_{\text{opt}} \\ &\quad + Q_{\text{opt}}A_{clj}^T < \tau I \qquad \text{for } i, j \in \{1, \ldots, 16\} \\ &\qquad Q > I. \end{aligned}$$

D. Results on the Experimental Setup

The synthesized LPV controller is compared with the varying gain H_∞ controller on the experimental setup, see Fig. 16.

Let us remind that the main concern is to control the web tension during all the winding process. We observe an improvement of the winding web tension with the LPV controller. The maximum web tension variation ($\Delta T/T$) is reduced from 9% (with varying gain H_∞ controller) to 5% (with LPV controller). Notice that this variation is about 30% with constant gain H_∞ controller and 75% with the decentralized PID control, commonly used in the industry (see [7]).

The LPV controller gives better results concerning the rejection of the velocity disturbances at the winding web tension. However, the winding web tension response for reference tracking is not completely satisfying. We observe a nonminimum phase-like response at the winder and the velocity response has a to high overshoot. The next step is to combine the two techniques: an LPV controller with multiplication by the radius.

VII. LPV Control With Varying Gains Depending on the Radius

Four H_∞ controllers are synthesized using the plant G_R. We proceed in the same way than in the previous section to implement the controller. We obtain globally the best performance with this controller. The amplitude of the web tension variations is about 4% for a variation of the velocity of 30%, and without overshoot of the velocity response, see Fig. 17.

To characterize the robustness of the different controllers we have synthesized, we compare the responses of web tensions and web velocity during simultaneous change in web tension and velocity. The first test consists into decreasing the traction motor velocity and, at the same time, increasing the winding tension and decreasing the unwinding web tension. The responses are plotted on the left on Fig. 18. We can see that the performances of the unwinding tension responses are almost the same with the different controllers. But very poor performances are obtained on the winding tension responses with the H_∞ and LPV controllers. The best response is obtained using the LPV controller with the multiplication by the radius, with the shortest stabilization time around the final value. The same remark can be done for the velocity responses.

The second test consists into decreasing the traction motor velocity and, at the same time, increasing the unwinding tension and decreasing the winding tension. The responses are plotted on the right on figure Fig. 18. The difference between the two controllers with multiplication by the radius is less significant.

The responses with the PID controllers are not represented and obviously are the worst. We observe with PID controllers, web sliding on the traction motor roll of our experimental setup despite its very sticking surface.

Finally, we can conclude the following.

- The H_∞ controller synthesized around a nominal point corresponding to the starting phase guarantees a good starting phase but exhibits poor performance during the end of the winding process.
- The LPV controller has good properties of disturbance rejection but is not efficient for reference tracking.
- The H_∞ controller with multiplication by the radius has fair performance concerning reference tracking and disturbance rejection and its implementation remains simple.
- The LPV controller with multiplication by the radius has very good performance concerning the reference tracking and disturbance rejection, but is of much higher order.

VIII. Conclusion

Web winding systems require an efficient control of the web tension during all the process operation. However, the radius and the inertia of the rollers vary on a large scale, therefore, changing considerably the system dynamics.

A model is built and identified in order to study the properties of the system and to synthesize advanced controllers. A multivariable approach significantly reduces the coupling between the web tension and the web velocity. But, to preserve the same performance during all the winding process, the controller needs to be adapted to the operating points. The first approach uses a particularity of the plant model by introducing the radius of the rollers as proportional gains in the controller. A H_∞ controller with varying gains depending on the radius allows to improve the performance during the winding process operation.

To further improve stability and performance an LPV controller is proposed which has the vertices synthesized for the operating points corresponding to the minimum and maximum of the radius. The stability of the closed-loop system is guaranteed for all admissible parameter trajectories and the performance is almost the same during all the process operation (on the nominal trajectory). The LPV controller does not bring a significant improvement on the H_∞ controller with varying gains. However, an LPV controller with varying gains depending on the radius gives extremely good results.

Last but not least, it should be noted that all the controllers are validated on a real experimental setup.

Appendix

TABLE I
Parameters of the Experimental Setup

Nominal torque of unwinding/winding brushless motors	6.8 Nm
Nominal velocity of unwinding/winding brushless motors	3000 rpm
Nominal torque of traction brushless motor	2.6 Nm
Nominal velocity of traction brushless motor	3000 rpm
Total length between winder and unwinder	1.9 m
Web width	0.1 m
Web thickness	0.275 mm
Diameter of full roll	0.2 m
Young modulus of the web	0.16 10^9 N/m^2
Nominal web tension	1.5 kg
Nominal web velocity	100 m/min
Maximum web velocity	500 m/min

References

[1] K. N. Reid and K.-C. Lin, "Control of longitudinal tension in multi-span web transport systems during start-up," in *Proc. Int. Conf. Web Handling IWEB2*, 1993, pp. 77–95.

[2] W. Wolfermann, "Sensorless tension control of webs," in *Proc. Int. Conf. Web Handling IWEB4*, 1997.
[3] ——, "Tension control of webs. A review of the problems and solutions in the present and future," in *Proc. Int. Conf. Web Handling IWEB3*, 1995, pp. 198–229.
[4] S. H. Jeon, J.-M. Kim, K.-C. Jung, S.-K. Sul, and J. Y. Choi, "Decoupling control of briddle rolls for steel mill drive system," *IEEE Trans. Ind. Applicat.*, vol. 35, pp. 119–125, 1999.
[5] J. E. Geddes and M. Postlethwaite, "Improvements in product quality in tandem cold rolling using robust multivariable control," *IEEE Trans. Contr. Syst. Technol.*, vol. 6, pp. 257–267, 1998.
[6] M. J. Grimble, *Advances in Control—Advanced Control for Hot Rolling Mills*. London, U.K.: Springer-Verlag, 1999, Highlights of ECC'99.
[7] H. Koç, D. Knittel, M. de Mathelin, and G. Abba, "Robust control of web transport systems," in *Proc. IFAC Symp. Robust Contr. Design ROCOND'00*, 2000.
[8] H. Noura, D. Sauter, F. Hamelin, and D. Theilliol, "Fault tolerant control in dynamic systems: Application to a winding machine," *IEEE Contr. Syst. Mag.*, pp. 33–49, Feb. 2000.
[9] P. Apkarian, J.-M. Biannic, and P. Gahinet, "Self-scheduled H_∞ control of missile via linear matrix inequalities," *J. Guid. Contr., Dyn.*, vol. 18, pp. 532–538, 1995.
[10] S. Bittanti, F. A. Cuzzalo, M. Lovera, and N. Lussana, "An LPV-LMI approach to generalized active control of vibrations in helicopters," in *Proc. Europ. Contr. Conf. ECC'99*, 1999.
[11] H. Kajiwara, P. Apkarian, and P. Gahinet, "LPV techniques for control of an inverted pendulum," *IEEE Contr. Syst.Mag.*, vol. 19, pp. 44–54, 1999.
[12] G. Brandenburg, "Ein mathematisches Modell für eine durchlaufende elastische Stoffbahn in einem System angetriebener, umschlungener, Walzen," *Regelungstechnik und Prozess-Datenverarbeitung*, vol. 3, pp. 69–162, 1973.
[13] H. Koç, D. Knittel, G. Abba, M. de Mathelin, C. Gauthier, and E. Ostertag, "Modeling and control of an industrial accumulator in a web transport system," in *Proc. Europ. Contr. Conf. ECC'99*, 1999.
[14] H. Koç, D. Knittel, M. de Mathelin, G. Abba, and C. Gauthier, "Web tension control in an industrial accumulator," in *Proc. Int. Conf. Web Handling IWEB5*, 1999.
[15] H. Koç, "Modélisation et commande robuste d'un système d'entraînement de bande flexible," Ph.D. dissertation, Strasbourg I Univ., France, Sept. 2000.
[16] K.-H. Shin, "Distributed control of tension in multi-span web transport systems," Ph.D. dissertation, Oklahoma State Univ., Oklahoma City, OK, 1991.
[17] E. Walter and L. Pronzato, *Identification of Parametric Models From Experimental Data*. New York: Springer-Verlag, 1997.
[18] T. Bastogne, H. Houra, P. Sibille, and A. Richard, "Multivariable identification of a winding process by subspace methods for tension control," *Contr. Eng. Practice*, vol. 6, pp. 1077–1088, 1998.
[19] S. Skogestad and I. Postlethwaite, *Multivariable Feedback Control*. Reading, MA: Addison-Wesley, 1996.
[20] H. Kwakernaak, "Robust control and H_∞ optimization—Tutorial paper," *Automatica*, vol. 29, pp. 255–273, 1993.
[21] K. Zhou, J. Doyle, and K. Glover, *Robust and Optimal Control*. Upper Saddle River, NJ: Prentice-Hall, 1996.
[22] R. W. Beaven, M. T. Wright, and D. R. Seaward, "Weighting function selection in the H_∞ design process," *Contr. Eng. Practice*, vol. 4, pp. 625–633, 1996.
[23] P. Apkarian and P. Gahinet, "A convex characterization of gain-scheduled H_∞ controllers," *IEEE Trans. Automat. Contr.*, vol. 40, pp. 853–864, 1995.
[24] P. Apkarian, P. Gahinet, and G. Becker, "Self-scheduled H_∞ control of linear parameter varying systems: A design example," *Automatica*, vol. 31, pp. 1251–1261, 1995.
[25] P. Apkarian, E. Feron, and P. Gahinet, "Parameter-dependant Lyapunov functions for robust control of systems with real parametric uncertainty," in *Proc. Europ. Contr. Conf. ECC'95*, vol. 3, 1995, pp. 2275–2280.
[26] P. Gahinet, A. Nemirovski, A. J. Laub, and M. Chilali, *LMI Control Toolbox*. Natick, MA: The Math Works Inc., 1995.
[27] H. Koç, D. Knittel, M. de Mathelin, and G. Abba, "Robust gain-scheduling control in web winding systems," in *Proc. IEEE Conf. Decision Contr.*, 2000.

Hakan Koç was born in Turkey in 1974. He moved with his family to France in 1983. He received the Ph.D. degree in automatic control from Strasbourg I University, Stasbourg, France, in 2000.

Currently, he lives in Germany and works for SIEMENS AG in the Application Center for Production Machines of the Division Automation and Drives. His interests include modeling, simulation, and application of advanced control strategies, particularly robust control, to industrial systems mainly in the domain of winding, printing, and packing.

Dominique Knittel received the Engineering diploma from the "Ecole Nationale Supérieure de Physique de Strasbourg," in 1987 and the Ph.D. degree from the University of Strasbourg in 1990, both in automatic control. Since 1992, he has been at the University of Strasbourg, where he is currently an Associate Professor.

Since 1999, he has been the team manager of the ERT Project "High speed handling and winding of flexible webs." His research interests include modeling, identification, robust control, control of large-scale systems, mainly for winding systems.

Michel de Mathelin received the Bachelor's degree in electrical engineering from Louvain University, Louvain-La-Neuve, Belgium, in 1987. He received the M.S. and Ph.D. degrees in electrical and computer engineering from Carnegie Mellon University, Pittsburgh, PA, in 1988 and 1993, respectively.

He was a Research Scientist in the Electrical Engineering Department of the Polytechnic School of the Royal Military Academy, Brussels, Belgium, during the 1991–1992 academic year. In 1993, he became Maître de Conférences at the Université Louis Pasteur (Strasbourg I University), Strasbourg, France. Since 1999, he has been Professor at the Ecole Nationale Supérieure de Physique de Strasbourg (ENSPS). His research interests include robust control, adaptive control, and robotics.

Dr. de Mathelin is a Fellow of the Belgian American Educational Foundation.

Gabriel Abba joined the "Ecole Normale Supérieure de Cachan," France, in 1979, and received the "agrégation" of Ministry of Education in electrical engineering in 1982. He received the Doctorate degree in electronics and robotics from the University of Paris XI-Orsay, Paris, France, in 1986.

Since 1999, he has been a Professor at the University of Metz and the head of the Industrial System and Maintenance Department. His research interests include development, modeling and control of robots, especially control of legged robots, visual serving, and control of high-speed drive for industrial applications.